Mutation Research 756 (2013) 66–77

Contents lists available at ScienceDirect

Mutation Research/Genetic Toxicology and Environmental Mutagenesis

journal homepage: www.elsevier.com/locate/gentox
Community address: www.elsevier.com/locate/mutres

Relative proximity of chromosome territories influences chromosome exchange partners in radiation-induced chromosome rearrangements in primary human bronchial epithelial cells☆

Helen A. Foster[a,b], Gemma Estrada-Girona[a,b], Matthew Themis[a,b], Elisa Garimberti[a,b], Mark A. Hill[c], Joanna M. Bridger[a], Rhona M. Anderson[a,b,*]

[a] Centre for Cell and Chromosome Biology, Division of Biosciences, Brunel University, West London UB8 3PH, UK
[b] Centre for Infection, Immunity and Disease Mechanisms, Division of Biosciences, Brunel University, West London UB8 3PH, UK
[c] CRUK/MRC Gray Institute for Radiation Oncology & Biology, Department of Oncology, University of Oxford, OX3 7DQ, UK

ARTICLE INFO

Article history:
Received 5 June 2013
Accepted 6 June 2013
Available online 18 June 2013

Keywords:
Complex chromosome exchanges
α-Particles
Nuclear geometry

ABSTRACT

It is well established that chromosomes exist in discrete territories (CTs) in interphase and are positioned in a cell-type specific probabilistic manner. The relative localisation of individual CTs within cell nuclei remains poorly understood, yet many cancers are associated with specific chromosome rearrangements and there is good evidence that relative territorial position influences their frequency of exchange. To examine this further, we characterised the complexity of radiation-induced chromosome exchanges in normal human bronchial epithelial (NHBE) cells by M-FISH analysis of PCC spreads and correlated the exchanges induced with their preferred interphase position, as determined by 1/2-colour 2D-FISH analysis, at the time of irradiation. We found that the frequency and complexity of aberrations induced were reduced in ellipsoid NHBE cells in comparison to previous observations in spherical cells, consistent with aberration complexity being dependent upon the number and proximity of damaged CTs, *i.e.* lesion proximity. To ask if particular chromosome neighbourhoods could be identified we analysed all radiation-induced pair-wise exchanges using SCHIP (statistics for chromosome interphase positioning) and found that exchanges between chromosomes (1;13), (9;17), (9;18), (12;18) and (16;21) all occurred more often than expected assuming randomness. All of these pairs were also found to be either sharing similar preferred positions in interphase and/or sharing neighbouring territory boundaries. We also analysed a human small cell lung cancer cell line, DMS53, by M-FISH observing the genome to be highly rearranged, yet possessing rearrangements also involving chromosomes (1;13) and (9;17). Our findings show evidence for the occurrence of non-random exchanges that may reflect the territorial organisation of chromosomes in interphase at time of damage and highlight the importance of cellular geometry for the induction of aberrations of varying complexity after exposure to both low and high-LET radiation.

1. Introduction

Determination of the complexity of radiation-induced chromosome aberrations has been widely examined since the application of whole chromosome painting techniques demonstrated the occurrence of complex chromosome aberrations (3 or more breaks in 2 or more chromosomes) to be more common than previously thought [1]. 24-Colour and multiple-colour banding techniques have since provided insight into the characteristic induction of complex exchanges after exposure to low doses of high-linear energy transfer (LET) radiation and also after relatively high doses of low-LET radiation, revealing their importance not just as potential biomarkers of radiation exposure and determinants for cellular fate [2–6], but also as events that further our understanding of the mechanisms of chromosome exchange formation. For instance, by combining multiplex-fluorescence *in situ* hybridisation (M-FISH) data of complex aberrations with modelling predictions of the number of chromosome territories (CTs) intersected by individual α-particle tracks, a correlation between aberration complexity and the number of individual territories intersected by each track was shown [7]. A model was proposed which was based on theoretical 'rejoining' cycles [8–10] whereby complex exchanges could

* Corresponding author at: Centre for Cell and Chromosome Biology, Division of Biosciences, Brunel University, West London UB8 3PH, UK. Tel.: +44 1895 267138.
E-mail address: Rhona.anderson@brunel.ac.uk (R.M. Anderson).

1383-5718/$ – see front matter © 2013 The Authors. Published by Elsevier B.V. All rights reserved.
http://dx.doi.org/10.1016/j.mrgentox.2013.06.003

theoretically be formed through sequential linking of smaller, independent exchanges [11] inferring that aberrations of increasing complexity are cumulative products of multiple, localised rearrangements [7,12]. This implies two important aspects that relate to chromosome aberration formation. Firstly, for particulate exposure, aberration complexity is a consequence of the number of different CTs intersected by each track and therefore is related to the geometry of the nucleus and the angle of irradiation and secondly, for all radiations, aberration complexity is related to the likelihood that individual, localised rearrangements sequentially link and so highlights the importance of ionisation density and lesion proximity throughout the nuclear space [13,14].

Chromosome aberrations are visualised routinely in mitosis when chromosomes are in a condensed state however, the damage and repair which result in the formation of chromosome aberrations occur during the interphase stage of the cell cycle. 2 dimension (D) and 3D interphase FISH technology [15,16] enables the tertiary organisation of chromosomes in interphase to be examined, for example for the determination of the relative localisation of individual CTs within the cell nucleus [17,18]. The application of these techniques is especially relevant for the study of how radiation-induced chromosome aberrations may be formed and also for understanding radiation-induced carcinogenesis since the nature of ionising radiation leads to correlation of interaction events and, therefore, initial damage along individual radiation tracks. This is important given that many cancers are associated with specific chromosome rearrangements and that there is good evidence associating the relative territorial position of certain chromosomes with their exchange frequency [19–23].

To examine this further and gain insight into physical mechanisms associated with the formation of chromosome rearrangements, we characterised the complexity of radiation-induced chromosome exchanges induced in a normal human lung cell type and correlated the chromosome exchange partners involved with their preferred interphase position at the time of irradiation. Our findings support the premise that aberration complexity is related, in part, to the number of CTs intersected. We also show certain chromosome pairs to occupy neighbouring territories in interphase nuclei and that this physical proximity influences their likelihood of forming a chromosome exchange.

2. Methods

2.1. Cell culture and irradiation of primary normal human bronchial epithelial cells

We sourced normal human bronchial epithelial cells (NHBE cells) commercially (Lonza is an FDA approved tissue bank). They had been isolated from human donor (Lot number 6F4181) with full donor consent. NHBE cells were maintained at 37 °C in a gassed incubator (5% CO_2/95% air) in T75 flasks at a density of 3.5×10^3 cells/cm^2 in 15 ml complete Bronchial Epithelial cell Basal Medium (BEBM) (Lonza Bullet kit CC-3170; BEBM is supplemented with retinoic acid (0.1%), human epidermal growth factor (0.1%), epinephrine (0.1%), transferrin (0.1%), triiodothyronine (0.1%), insulin (0.1%), hydrocortisone (0.1%), bovine pituitary extract (0.2%) and gentamicin/amphotericin-B (0.1%) by addition of SingleQuots™ (Lonza)). Cells were passaged between 80 and 90% confluence (generally ~4 days in culture (~$1–1.5 \times 10^6$ cells total)), as recommended by the supplier, and re-fed every 48 h. For this, medium was removed and the cell sheet washed in HEPES buffer before addition of ~6 ml of trypsin/EDTA solution (0.25 μg/ml) for ~4 min, followed by the addition of 12 ml trypsin neutralising solution (TNS) (Lonza). Cells were centrifuged at 220 g for 5 min then re-suspended in complete BEBM. Cells were frozen in 10% DMSO for long term storage from passage 3 (p3).

For γ-irradiations, NHBE cells were irradiated at room temperature (RT) as a monolayer at 80–90% confluency using the ^{60}Co source at Brunel University at 37 °C at dose rate of 0.0944 Gy/min. For α-particle irradiations, the NHBE cells were passaged and seeded onto Hostaphan-based (0.35 mg cm^{-2} polyethylene terephthalate; Hoeschst, Weisbaden, Germant) glass-walled dishes (30 mm internal diameter) for 24 h and then transferred, in a portable incubator at 37 °C, to the Gray Institute for Radiation Oncology & Biology in Oxford. The cells were then maintained in a humidified gassed (5% CO_2/95% air) incubator at 37 °C as standard for a further 24–48 h before being irradiated at RT as a monolayer at 80–90% confluency (~$1.2–1.5 \times 10^5$ cells/dish) with 3.26 MeV α-particles (LET of 121 keV/μm) using a ^{238}Pu α-particle irradiator described previously [24]. Cells were exposed to a dose of 0.19 Gy (~0.1 Gy/min) which corresponds to a mean of 1.03 high-LET α-particle traversals per cell nucleus for a nuclear area of 105 μm^2 (actual number of nuclear traversals follows a Poisson distribution where 35.7%, 36.8%, 18.9% and 8.6% of nuclei are traversed by 0, 1, 2 or ≥3 tracks).

2.2. Collection of metaphase and prematurely condensed chromosome (PCC) spreads from NHBE cells

We elected to irradiate early passage NHBE (p3/p4) cells in an effort to more closely mimic effects in 'primary' cells rather than in populations that have been repeatedly passaged *in vitro*. However the total number of cells available for experimentation at early passage is limited and insufficient for suspension harvest methodology. In addition, preliminary experiments showed NHBE cells to be refractory to standard colcemid treatment for the collection of mitotic chromosomes with mitotic indices achieved of <1%. Accordingly, irradiated cells were seeded onto glass microscope slides for culture and treatment for the premature condensation of chromosomes (PCC) *in situ*.

NHBE cells were seeded and irradiated with either low-LET γ-rays or high-LET α-particles as a monolayer at 80–90% confluency as described in Section 2.1. After irradiation, NHBE cells were allowed to recover for 1 h at 37 °C then passaged and seeded at a density of 3.5×10^3 cells/cm^2 in fresh complete BEBM, containing 10 μM 5′-bromodeoxyuridine (BrdU), onto flame sterilised glass microscope slides housed within individual quadriperm chambers (Starsted). The cells were then cultured for finite periods of time and harvested to achieve the optimal collection of 1st post-irradiation metaphases by adding 40 ng/ml demecolchicine for the final 5 h of the culture time. Calyculin A (50 nM) was added 30 min before fixation to induce PCC in G_2 cells. The medium was then discarded and the cells incubated in hypotonic solution (0.075 M KCl) at 37 °C for 15 min before being fixed by gently washing the microscope slides with fresh ice-cold 3:1 (v/v) methanol:acetic acid for ~3–5 min. Slides were dried individually on a humidified hot-plate to obtain well spread quality chromosome preparations and stored in an air-tight container containing silica gel at −20 °C until required.

2.3. Cell culture and preparation of metaphase chromosomes of DMS53 cell line

DMS53, a human small cell lung cancer (SCLC) cell line was obtained from the European Collection of Cell Cultures (ECACC, Salisbury, UK) and cultured in Waymouth's Medium MB 752/1 (Lonza) supplemented with 10% (v/v) of heat inactivated FBS and 1% penicillin/streptomycin/glutamine at 37 °C in 5% CO_2/95% air. Cells were harvested to obtain mitoses by the addition of 0.025 μg/ml demecolchicine (Gibco) for the last 18 h of a total of 48 h culture period prior to being trypsinized and harvested from the flasks. The cell suspension was centrifuged at 200 × *g* for 5 min and re-suspended in ~8 ml of hypotonic solution (1:1 of potassium chloride (0.075 M):sodium citrate (0.9%)) for 7 min at 37 °C. The cells were centrifuged once more and then re-suspended in a drop-wise fashion in fresh ice-cold 3:1 (v/v) methanol:acetic acid, left for ~1 h at −20 °C, fixed a further 4–5 times in fresh fixative solution and stored at −20 °C until required.

2.4. Multiplex fluorescence in situ hybridisation (M-FISH) assay

A modified method of the Metasystems™ protocol was used. To do this, fresh slides of chromosome preparations were hardened (3:1 methanol:acetic acid for 1 h, dehydrated through an ethanol series (2 min each in 70%, 70%, 90%, 90% and 100%), baked at 65 °C for 20 min, then 10 min in acetone) before being pre-treated with RNase A (100 μg/ml in 2× SSC) at 37 °C for 1 h and then washed in 2× SSC.

For hybridisation, 10 μl of Metasystems™ 24-colour probe cocktail was denatured by incubating at 75 °C for 5 min. After this time, the probe was placed onto ice briefly then incubated at 37 °C for 30 min. In parallel, slides were incubated in 0.1× SSC for 1 min at RT, 2× SSC for 30 min at 70 °C and 0.1× SSC for 1 min at RT. The slides were then denatured in 0.07 N NaOH for 1 min at RT, before being washed sequentially in 0.1× SSC at 4 °C and 2× SSC at 4 °C for 1 min each and dehydrated through an ethanol series of 30, 50, 70, and 100% for 1 min each. Cells and probe were then mixed, overlayed with a pre-warmed coverslip and left to hybridise for 48–72 h at 37 °C before being washed in 1× SSC at 73 °C for 5 min and 4× SSC/0.05% Tween 20 at RT for 5 min. A mix of 50 μl blocking reagent containing 1 μl Metasystems™ detection agent was then applied to the slide and overlayed using a coverslip and incubated at 37 °C for 15 min. After this time, the slide was washed sequentially in 4× SSC Tween 20 and PBS at RT for 3 min each, then left to dry in the dark at RT. Cells were counterstained using 4′,6-diamidino-2-phenylindole (DAPI III) (Vysis, UK), sealed and stored in the dark at −20 °C.

2.4.1. M-FISH analysis

Chromosome aberrations were analysed as previously described [2]. In brief, PCC spreads were visualised using an 8-position Zeiss Axioplan II fluorescence microscope containing individual filter sets for each component fluor of the Metasystems™ probe cocktail plus DAPI. Digital images were captured for M-FISH using a charged-coupled device (CCD) camera (Photometrics Sensys CCD) coupled to and driven by ISIS (Metasystems™). In the first instance, cells were karyotyped and

analysed by enhanced DAPI banding. Detailed paint analysis was then performed by assessing paint coverage for each individual fluor down the length of each individual chromosome, using both the raw and processed images for each fluor channel. A PCC spread was classified as being apparently normal if all 46 chromosomes were observed by this process, and subsequently confirmed by the Metasystems™ M-FISH assignment, to have their appropriate combinatorial paint composition down their entire length.

2.4.2. Classification of chromosome aberrations

Structural chromosomal abnormalities were identified as colour-junctions down the length of individual chromosomes and/or by the presence of chromosome fragments. The M-FISH paint composition was used to identify the chromosomes involved in the abnormality and assignment of a breakpoint to a specific chromosomal region (pter, p, peri-centromere, q or qter) was based on the DAPI banding pattern at the M-FISH colour junction, the location of the centromere and the size of the painted material on each rearranged chromosome.

For radiation-induced aberrations in NHBE cells, exchange aberrations involving three or more breaks in two or more chromosomes were classed as *complex*, while those involving only two breaks in one or two chromosomes were classified as *simple*. To test for any non-random chromosome exchanges, colour-junctions between participating chromosomes were identified in all simple and complex aberrations. For each exchange, each colour-junction was only scored once. For DMS53, abnormalities were described according to International System of Cytogenetic Nomenclature [65].

2.5. Interphase chromosome territory positioning in NHBE cells using 2D-FISH with whole chromosome paints (WCP)

2.5.1. Cell culture and fixation

To correlate the preferred territorial position of chromosomes with chromosome exchange aberrations induced upon exposure to ionising radiation, populations of un-irradiated NHBE cells were cultured using the same conditions as described in Section 2.1. Cells were trypsinised at 80–90% confluence and the cell suspension centrifuged at 200 × *g* for 5 min before being re-suspended in ~7 ml hypotonic buffer (0.075 M KCl) and being left at room temperature for 15 min. The cells were centrifuged once more and fixed by the drop-wise addition of fresh ice-cold 3:1 (v/v) methanol:acetic acid with constant agitation. After an incubation period of a minimum of 1 h at 4 °C, the cells were washed an additional two times with fresh 3:1 fixative, 'dropped' onto slides and stored in an air-tight container containing silica gel at −20 °C until required.

2.5.2. Whole chromosome paint (WCP) preparation

Whole human chromosome paints for chromosomes 1, 7, 9, 10, 12, 13, 16, 17, 18 and 21 were created. These were generated from micro-dissected normal chromosome arm templates (a kind gift to Joanna Bridger from Michael Bittner). Degenerate oligonucleotide primed PCR (DOP-PCR) was used initially to amplify the micro-dissected template and then to create probes by labelling with either digoxigenin-11-dUTP (Roche) or biotin-16-dUTP (Roche). For amplification, chromosome template was mixed with a final concentration of 1× KAPA HiFi Fidelity Buffer (KAPA Biosystems), 0.2 mM dNTP mix, 2 μM DOP primer, 0.02 U/μl Taq polymerase and sterile water. The thermal cycling conditions were initial denaturation at 95 °C for 3 min followed by 31 cycles of denaturation (98 °C), annealing (62 °C) and extension (72 °C) for 20 s, 1 min and 30 s each, with a final extension at 72 °C for 5 min. Amplified product was then labelled using the aforementioned conditions with the exception that a final concentration of 80 μM dTTP was used with either 0.2 mM digoxigenin-11-dUTP or 0.2 mM biotin-16-dUTP. A total of 34 cycles of denaturation, annealing and extension was carried out.

200–400 μg of digoxigenin or biotin labelled DNA was mixed with 7 μg of Cot1 DNA, 30 μg herring sperm DNA, 1.8 μl 3 M sodium acetate and 40 μl ice-cold 100% ethanol, then incubated at −80 °C for a minimum of 30 min before being centrifuged at 500 × *g* for 30 min at 4 °C. After removing the supernatant, the DNA pellet was washed with 200 μl of ice-cold 70% ethanol and centrifuged again at 500 × *g* for 15 min at 4 °C. The supernatant was removed and the pellet dried at 37 °C before being dissolved in 12 μl of hybridisation mix (10% dextran sulphate, 2× SSC, 50% formamide, 1% Tween 20,) for at least 2 h at 50 °C.

2.5.3. Slide and WCP denaturation

Slides were baked at 70 °C for 1 h, dehydrated through an ethanol series (70, 90, and 100%) and dried at 70 °C for a further 5 min. To denature chromosomes, slides were immersed in 70% formamide in 2× SSC at 70 °C for 2 min then immediately quenched in ice-cold 70% ethanol for 5 min. The slides were then dehydrated through 90 and 100% ethanol for 5 min each and dried on a warming plate. Probes were denatured by incubating at 75 °C for 10 min followed by pre-annealing at 37 °C for 45 min before being applied onto the denatured slide. The probe was then overlayed with a pre-warmed coverslip, sealed and left to hybridise overnight in a humidified chamber at 37 °C.

2.5.4. Post-hybridisation washes and detection

The sealant was carefully removed and the slides washed three times in 50% formamide in 2× SSC at 45 °C for 5 min each with gentle agitation. The slides were then washed three times in 0.1× SSC (preheated to 60 °C) at 45 °C for 5 min each followed by 4× SSC at RT for 5 min. For post-hybridisation detection, the procedure from Garimberti and Tosi was used [25]. Briefly, each slide was incubated with 100 μl of 3% bovine serum albumin (BSA) in 4× SSC at RT for 1 h at 37 °C to block any non-specific binding. After this time, 100 μl of 20 μg/ml Cy-3 strepavidin (GE Healthcare) and/or mouse anti-digoxigenin (diluted 1:666) (Sigma–Aldrich) in 3% BSA in 4× SSC/0.05% Tween 20 and was applied onto each slide, overlayed with a coverslip and incubated in the dark for 30 min at 37 °C in a humidified chamber. The slides were then washed three times by shaking in 4× SSC/0.05% Tween 20 for 3 min each at RT in the dark. For digoxigenin-labelled WCPs, 100 μl of rabbit anti-mouse-FITC (Sigma–Aldrich) diluted 1:1000 with 3% BSA in 4× SSC/0.05% Tween 20 was applied, overlayed with a coverslip and incubated once more in the dark in a humidified chamber at 37 °C for 20 min. This was followed by washing three times in 4× SSC/0.05%Tween 20 in the dark for 3 min each and then incubating with 100 μl of a 1:100 of monoclonal anti-rabbit-FITC (Sigma–Aldrich) at 37 °C for 20 min. After biotin and digoxigenin detection, the slides were washed twice with 4× SSC/0.05% Tween 20 for 3 min each and then washed once with 1xPBS for 5 min. The slides were briefly rinsed with water before being air dried and mounted with Vectashield containing DAPI™.

2.5.5. Combined FISH and immunofluorescence staining

A similar procedure to that described above was used to co-stain FISH preparations (labelled with biotin-dUTP) for the proliferative marker, Ki-67. After slides had undergone the post-hybridisation washes (Section 2.5.4) they were incubated in 4× SSC at RT for 5 min and blocked for 10 min at RT in 100 μl of 3% BSA in 4× SSC. 20 μg/ml Cy-3 strepavidin (GE Healthcare) in 1% BSA/4× SSC was applied to each slide and incubated in the dark at 37 °C for 30 min in a humidified chamber. After this time, the slides were washed three times in 4× SSC/0.05% Tween 20 for 5 min each at 42 °C then incubated with 100 μl of polyclonal rabbit anti-pKi-67 (Novacastra) at a 1:1500 dilution in 1% new-born calf serum (NCS)/PBS for 1 h at RT. Slides were then washed three times in PBS for 5 min each prior to being incubated with 100 μl of goat anti-rabbit AF488 diluted 1:200 in 1% NCS/PBS for 1 h at RT. Finally the slides were washed three times for 5 min each in PBS, rinsed briefly in water and mounted with Vectashield containing DAPI™.

2.5.6. Image acquisition and analysis

Slides were viewed using an Olympus BX41 fluorescence microscope and digital images captured using a Viewpoint GS digital camera (Digital Scientific) controlled by Digital Scientific Smart Capture3 software. 50 acquired images for each chromosome were then subjected to erosion chromosome position analysis by using a bespoke script, created by Dr Paul Perry, a kind gift of Prof Wendy Bickmore, MRC Human Genetics Unit, Edinburgh first published in 1999 [26]. The DAPI stain revealing the nucleus is delineated and then eroded inwards to create 5 shells of equal area. The intensity of the DNA (DAPI) signal and chromosome signal is then measured in each shell [26]. To normalise the data for the skewed distribution of DNA in a flattened nucleus the percentage chromosome intensity measurement is divided by the DAPI intensity measurement for each shell and the average for 50 images plotted in a histogram; the *y*-axis being the %chromosome signal/%DNA signal.

2.6. Interphase chromosome territory:chromosome territory measurements

Selected pairs of biotin-16-dUTP and digoxigenin-11-dUTP labelled WCPs were hybridised to un-irradiated NHBE nuclei and detected as described in Section 2.5. Slides were viewed using an Olympus BX41 fluorescence microscope and digital images captured using a Viewpoint GS digital camera (Digital Scientific) controlled by Digital Scientific Smart Capture3 software. 50 acquired images for each chromosome pair were then analysed in ImageJ software (National Institutes for Health (NIH), www.rsb.info.nih.gov) for the purpose of determining the average distance between homologous and heterologous chromosome territories (CTs). The distances between the boundary edges of each CT were measured.

3. Results

3.1. Exchange aberrations induced in NHBE cells after exposure to low-LET γ-rays and high-LET α-particles

Table 1 gives the frequencies and types of chromosome exchanges initially induced in NHBE cells after exposure to low-LET γ-rays and high-LET α-particles and shows that both simple and complex exchange types are induced (for more details see Themis et al. [27]). For γ-rays, the frequency of simple exchanges were significantly greater after exposure to 0.5 and 1 Gy compared to sham ($p < 0.004$) while a significantly greater frequency of complexes

Table 1
Frequency of exchange aberrations in NHBE cells visualised by M-FISH.

Test	Total cells	Damaged cells (frequency)	Type of damage (frequency)	
			Simple	Complex
Sham	490	0.112	6(0.010)	0(0.00)
0.5 Gy γ-rays	179	0.168	11(0.061)	2(0.011)
1.0 Gy γ-rays	106	0.217	11(0.104)	4(0.038)
~1 α-particle/nucleus	682	0.346	84(0.123)	42(0.062)

was induced again compared to sham (0.00) after exposure to 1 Gy (0.038, $p = 0.04$) but not 0.5 Gy (0.011, $p = 0.17$).

Simple and complex aberrations were also observed after exposure to ~1 α-particle/nucleus at frequencies of 0.123 and 0.062, respectively, giving a simple:complex (S:C) ratio of ~2 (Table 1). This proportion of complex aberrations induced is in contrast to previous α-particle studies at an equi-fluence of ~1 track/nucleus in peripheral blood lymphocytes (PBL) [7,12] and haemopoeitic stem cells (HSC) [28] where the S:C ratio was ~<1. In addition, only ~40% of NHBE cells classified as containing an exchange were found to have one or more complex, whereas this fraction was greater (60–80% depending on LET of the α-particle) for both PBL and HSC (Fig. 1). Therefore although complex chromosome aberrations were induced in NHBE cells exposed *in vitro* to high-LET α-particles they do not represent the dominant exchange-type when irradiated in a perpendicular set-up (*i.e.* through the base of the dish).

3.2. Interphase chromosome positioning in NHBE cells

To determine the preferred nuclear positioning of interphase chromosomes in NHBE cells we harvested and fixed a population of un-irradiated NHBE cells for 2D-fluorescence *in situ* hybridisation (FISH) using whole chromosome paints (WCP) for chromosomes 1, 7, 9, 10, 12, 13, 16, 17, 18 and 21. Digital images were subjected to erosion analysis and the data for each chromosome plotted as a histogram, with the *x*-axis displaying nuclear shells from 1 to 5 representing the nuclear periphery to the nuclear interior, respectively (Fig. 2) [26]. The *y*-axis is the percentage fluorescence signal intensity from the chromosome paint normalised by division with the percentage fluorescence signal intensity from the DAPI stained DNA.

When we visualise the erosion analysis data for chromosome positioning in the histograms (Fig. 2), the skew of the graph towards shell 1 or 5 allows us to state that the chromosome has a preferential position towards the nuclear periphery or interior, respectively. We find chromosomes 7, 10, 12, 13 and 18 preferentially located towards the nuclear periphery, chromosomes 16, 17 and 21 to occupy a more interior position and chromosome 1 to occupy an intermediate position. The histogram for chromosome 9 shows no apparent skew, instead it displays a bimodal distribution, implying that either each homologue is located in a different relative nuclear location or that there are two populations of cells within the culture. Although this bimodal distribution is seen only rarely in interphase chromosome positioning, the differential positioning of certain chromosomes has been observed in cells depending on their proliferative status [29,30]. For instance in fibroblasts, chromosome 18 is found in two different radial locations in Ki-67 positive and negative cells; with chromosome 18 at the nuclear periphery in positive proliferating cells and in the nuclear interior in negative non-proliferating cells. In addition, chromosome 9 also sits in two different locations in proliferating and non-proliferating cells (Bridger, unpublished data). Therefore, to assess whether a similar explanation accounted for the bimodal distribution of chromosome 9 in NHBE cells, we repeated the position analysis in cells co-stained with the cell proliferation marker anti-Ki-67 [31]. A similar staining strategy was carried out for chromosome 18, however, as Fig. 2 shows, we saw no difference in 2D positioning for either chromosome 9 or 18 between proliferative (Ki-67 positive) and non-proliferative (Ki-67 negative) cells. This suggests that NHBE cells do not reorganise their genomes when they become non-proliferating and that the bimodal distribution of chromosome 9 requires further examination.

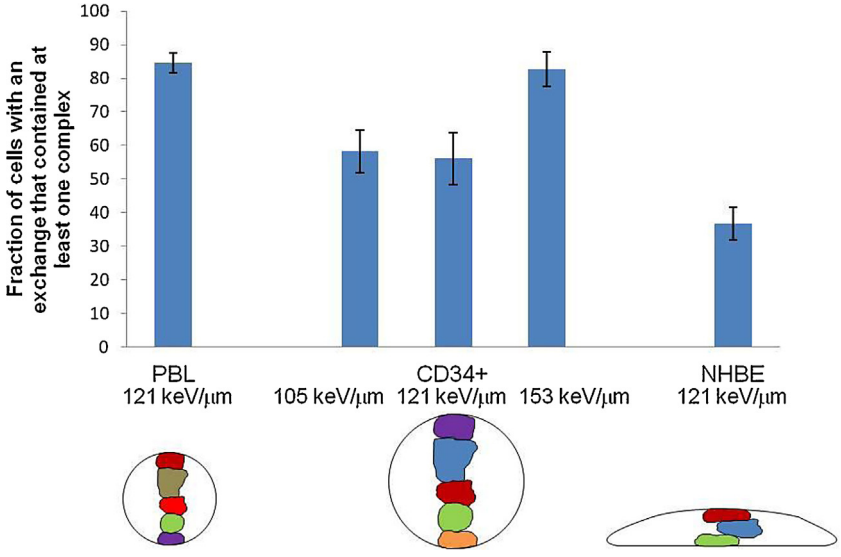

Fig. 1. Fraction of cells with an exchange that contained at least one complex. Data are shown for PBL [7], CD34$^+$ [28] and NHBE cells after exposure to ~1 α-particle/cell of varying incident LET. The relative differences in geometric shape and possible organisation of individual chromosome territories within each cell nuclei are shown.

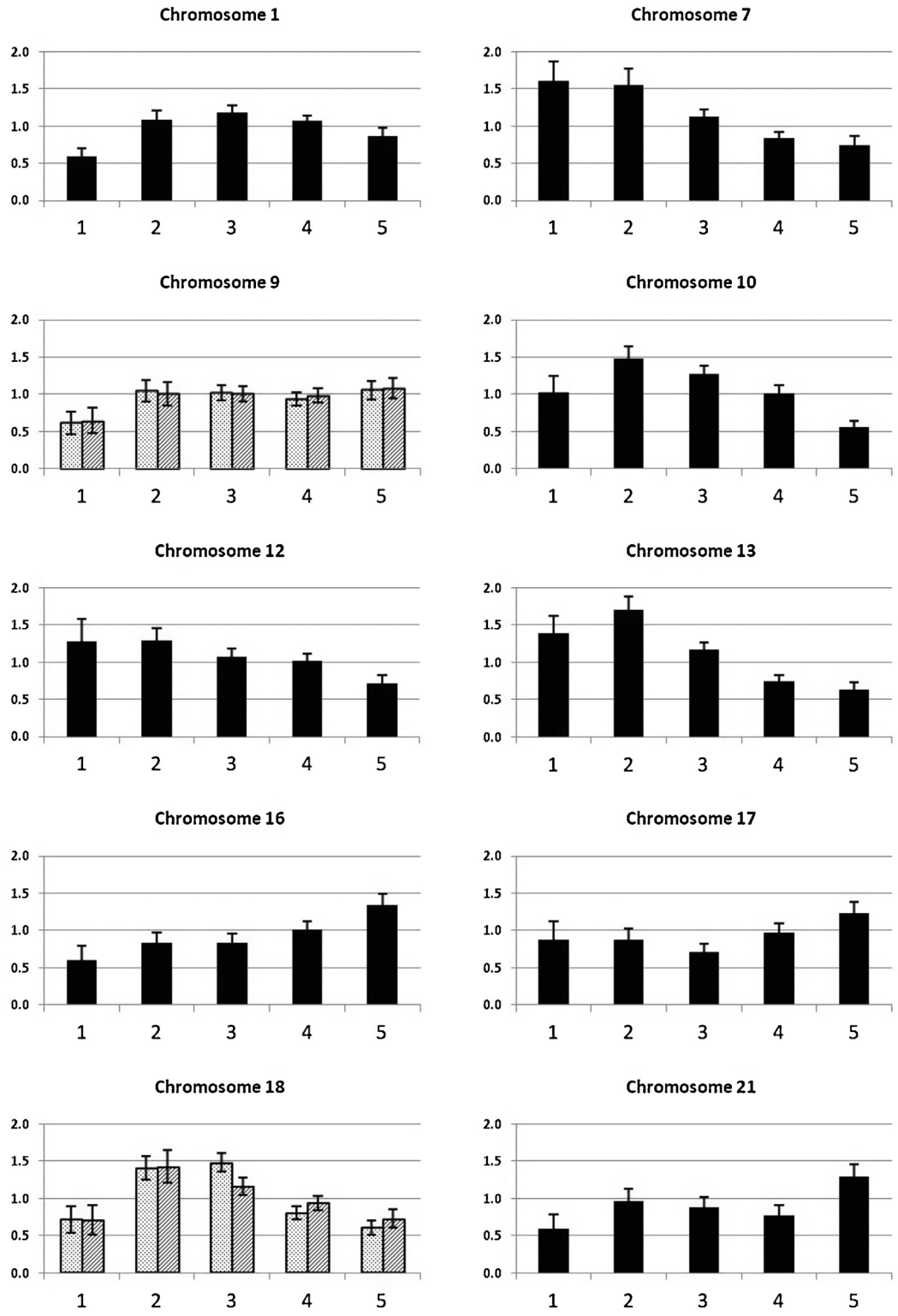

Fig. 2. 2D-FISH interphase chromosome position profiles in NHBE cells. For chromosomes 9 and 18, separate profiles were obtained for Ki-67 positive (dots) and Ki-67 negative (diagonals) populations. The *x*-axis shows 5 shells of equal area; shell 1 corresponds to the nuclear periphery and shell 5 corresponds to the nuclear interior. The *y*-axis shows the %chromosome signal/%DNA signal. 50 nuclei were analysed for each chromosome.

3.3. Determination of non-random chromosome exchange partners in NHBE cells

All chromosome exchange partners observed in 1st cell division metaphase + PCC spreads (Table 1) (identified by the presence of colour-junctions) were inserted into a triangular matrix (Table 2) for the purpose of identifying non-random associations between particular pairs of chromosomes. This was carried out by SCHIP (Statistics for Chromosome Interphase Positioning based on interchange data) analysis [32] which enables one to determine the deviation of the observed frequency of exchanges between chromosomes with respect to the expected frequency, assuming

Table 2
Triangular matrix of chromosome exchange partners observed in 1st cell division NHBE cells and SCHIP analysis data.

22	0	1	0	1	0	2	0	2	0	0	1	0	0	0	0	0	1	1	0	1	0	0.51
21	0	0	1	1	0	0	0	1	0	2	0	1	1	0	1	3	0	0	0	0	0.57	-0.54
20	0	1	1	1	1	1	0	0	0	1	1	0	0	0	0	0	0	0	0	0.41	-0.48	1.73
19	0	2	1	1	1	1	1	0	1	1	0	0	0	0	0	0	2	0	0.57	-0.48	-0.57	-0.54
18	0	0	0	1	1	1	1	0	3	1	1	5	1	1	0	0	1	0.94	-0.73	-0.62	-0.73	0.74
17	0	2	0	2	0	0	1	2	3	0	0	0	0	1	0	0	0.78	0.31	2.35	-0.56	-0.66	0.95
16	0	0	0	1	1	0	1	1	1	1	1	1	0	0	1	0.62	-0.69	-0.76	-0.59	-0.5	4.48	-0.56
15	1	1	3	0	0	0	2	1	0	1	0	1	2	1	0.78	0.74	-0.78	-0.86	-0.66	-0.56	0.84	-0.63
14	2	2	1	1	0	0	1	0	0	0	1	0	0	0.57	0.84	-0.59	0.84	0.64	-0.57	-0.48	-0.57	-0.54
13	4	2	0	0	2	0	2	1	0	0	1	2	0.94	-0.73	1.47	-0.76	-0.86	0.11	-0.73	-0.62	0.64	-0.7
12	1	2	2	4	1	2	1	2	0	1	1	1.46	0.53	-0.91	-0.13	0.1	-1.07	3.09	-0.91	-0.77	0.19	-0.86
11	1	1	1	0	2	0	1	1	1	2	0.89	-0.26	0.17	0.7	-0.83	0.61	-0.83	0.17	-0.71	1.06	-0.71	0.8
10	0	2	1	0	1	2	3	1	2	1.17	0.94	-0.54	-1.05	-0.81	0.09	0.33	-0.95	-0.1	0.42	0.76	1.65	-0.77
9	1	1	0	1	0	0	0	2	0.83	1.04	0.3	-1.1	-0.89	-0.69	-0.81	0.67	2.91	2.49	0.77	-0.58	-0.69	-0.65
8	2	1	2	1	0	4	0	1.28	0.9	-0.41	-0.13	0.1	-0.19	-0.85	0	0.23	1	-1.1	-0.85	-0.72	0.32	1.66
7	0	1	1	1	0	0	0.89	-1.07	-0.86	1.92	0.24	-0.26	1.27	0.7	1.57	0.61	0.37	0.17	0.7	-0.6	-0.71	-0.68
6	2	2	3	1	1	1.17	-1.02	2.05	-0.99	0.54	-1.02	0.23	-1.05	-0.81	-0.95	-0.85	-0.95	-0.1	0.42	0.76	-0.81	1.81
5	0	1	2	0	0.73	0.16	-0.8	-0.96	-0.78	0.16	1.69	-0.06	1.59	-0.64	-0.75	0.82	-0.75	0.38	0.92	1.29	-0.64	-0.61
4	1	1	1	1.06	-0.88	-0.21	0.06	-0.3	0.13	-1.11	-0.97	1.99	-1	0.52	-0.91	0.43	1.3	0	0.52	0.87	0.52	0.62
3	3	2	1.34	-0.35	1.04	1.15	-0.17	0.22	-1.06	-0.45	-0.17	0.04	-1.12	0.28	1.91	-0.91	-1.02	-1.12	0.28	0.61	0.28	-0.83
2	2	1.46	0.04	-0.43	-0.06	0.23	-0.26	-0.63	-0.19	0.23	-0.26	-0.08	0.53	1.3	-0.13	-0.95	0.81	-1.17	1.3	0.53	-0.91	0.29
1	1.06	0.37	1.33	-0.11	-0.88	0.69	-0.97	0.56	0.13	-1.11	0.06	-0.43	3.01	1.82	0.19	-0.81	-0.91	-1	-0.77	-0.66	-0.77	-0.74
Chr	**1**	**2**	**3**	**4**	**5**	**6**	**7**	**8**	**9**	**10**	**11**	**12**	**13**	**14**	**15**	**16**	**17**	**18**	**19**	**20**	**21**	**22**

The top half of the table shows the observed number of pair-wise exchanges between all heterologous autosomes and the bottom half shows the deviation from that expected if all the autosomes were randomly located relative to each other. A positive value indicates an excess of observed events, implying that two autosomes are, on average, closer to each other than expected [32].

Table 3
SCHIP analysis of selected pair-wise chromosome exchanges.

Candidate cluster	*p*-Value	Candidate cluster	*p*-Value
(1;2)	0.451200	(9;11)	0.527100
(1;3)	0.177300	**(9;17)**	**0.029300**
(1;13)	**0.019300**	**(9;18)**	**0.046500**
(1;18)	1.000000	**(12;18)**	**0.012200**
(3;6)	0.212800	(15;16)	0.383900
(3;15)	0.088300	**(16;21)**	**0.005000**
(4;12)	0.070300	(18;19)	1.000000
(6;8)	0.059500	(20;22)	0.187000
(6;10)	0.401500	(21;22)	1.000000
(7;10)	0.094500		

Bold font denotes statistical significance at 95%.

randomness. Although SCHIP cannot 'mine' interchange matrix tables to extract non-random pair-wise exchanges, it can be used to test the significance of particular 'chromosome clusters'. Accordingly, we identified the pair-wise exchanges that appear to occur more frequently than others based on data in the upper part of Table 2 as (1;3), (1;13), (3;6), (3;15), (4;12), (6;8), (7;10), (9;17), (9;18), (12;18) and (16;21). Given the small numbers of 'events' in our data-set due to the limited number of exchanges actually induced (Table 1) (essentially 202 colour-junctions distributed over 231 possible heterologous pair-wise combinations) we have also included a number of pair-wise exchanges that did not appear to occur with any frequency, specifically (1;2), (1;18), (6;10), (9;11), (15;16), (18;19), (20;22) and (21;22). Table 3 shows the *p*-values obtained for the above mentioned candidate clusters and identifies five radiation-induced pair-wise exchanges, namely (1;13), (9;17), (9;18), (12;18) and (16;21), that occur more often than expected assuming randomness. To examine these findings in more detail, 2-colour FISH was performed for the purpose of determining the distance between chromosome territories (CTs) for identified pairs of chromosomes (Fig. 3). The average distance between the visible edges of the two closest CTs was 0.21 ± 0.49 μm (range 0–2.06), 0.75 ± 0.99 μm (range 0–2.47) and 0.61 ± 0.94 μm (range 0–2.85) for chromosomes (1;13), (9;17) and (16;21) respectively (Table 4). In addition, 50–60% of all nuclei observed (for each pair) had at least one pair of CTs visibly touching and sharing neighbouring CT surfaces. By contrast the average distance between homologous pairs was >3.5 μm (Table 5) consistent with measurements reported by Zeitz et al. [33] and Heride et al. [34].

3.4. M-FISH karyotypic analysis of small cell lung cancer cell line DMS53

A causal relationship between Radon exposure in the home and the occurrence of lung cancer has been demonstrated, with estimates that Radon accounts for 9% of all lung cancer deaths in Europe [35,36]. The histological type that most contributed to this increase were small cell lung cancers (SCLC), therefore, a previously uncharacterised non-metastatic SCLC cell line (DMS53) was selected for M-FISH karyotypic analysis with the objective of identifying clonal aberrations that may reflect findings in NHBE cells.

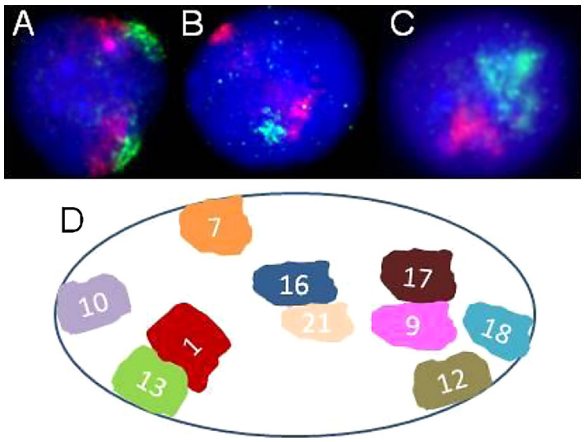

Fig. 3. Relative interphase positions of chromosomes in NHBE cells. Panel A shows chromosomes 1 (red) and 13 (green), Panel B shows chromosomes 9 (green) and 17 (red) while Panel C shows chromosomes 16 (red) and 21 (green). Panel D outlines a 'map' of the relative positioning of chromosome territories in NHBE cells as determined by combining information generated from chromosome position analysis, SCHIP analysis of radiation-induced aberrations and 2-colour FISH of CTs.

Table 5
Average distance between homologous chromosome pairs in interphase.

Chromosome	Average distances between CTs (μm)	Touching CTs (% of nuclei)
1–1	4.04 ± 2.54	7
9–9	5.42 ± 3.35	0
13–13	3.52 ± 2.54	1
16–16	5.66 ± 3.98	0
17–17	5.79 ± 2.81	0
21–21	3.25 ± 2.13	0

12 DMS53 cells were fully karyotyped revealing extraordinarily complex cytogenetic patterns (Fig. 4) with most metaphases displaying similar cytogenetic features and very few apparently normal chromosomes. For this reason, individual karyotypes were drawn in a cartoon format and grouped in an effort to identify those chromosomes that were interacting with each other (Fig. 5). By doing this for each metaphase spread a number of clonal abnormalities were identified (Tables 6 and 7).

4. Discussion

Both simple (S) and complex (C) aberrations were observed in NHBE cells after exposure to high-LET α-particles (~1 α-particle/nucleus) and low-LET γ-rays (1 Gy), however only simple exchanges were detected at appreciable levels above sham at the lower dose of 0.5 Gy γ-rays (Table 1), consistent with expectations that exposure to low doses of sparsely ionising radiation only rarely results in complex rearrangements (*e.g.* involving multiple breaks in two different chromosomes) [5]. The proportion of all exchanges classified as complex after exposure to high-LET α-particles was ~33% (S:C ratio ~2), in-line with that observed in fibroblast cells [22,37,38] but in contrast to previous M-FISH studies examining

Table 4
Average distances between heterologous chromosome pairs in interphase.

Chromosome pair	Average distances between CTs in order of relative proximity (μm)				
	1		2	3	4
		Touching CTs (% of nuclei)			
1 and 13	0.21 ± 0.49	59	1.7 ± 1.62	4.69 ± 1.69	7.09 ± 2.12
9 and 17	0.75 ± 0.99	64	2.7 ± 2.21	5.38 ± 2.87	8.59 ± 2.57
16 and 21	0.61 ± 0.94	51	2.74 ± 2.48	4.54 ± 2.43	6.7 ± 3.08

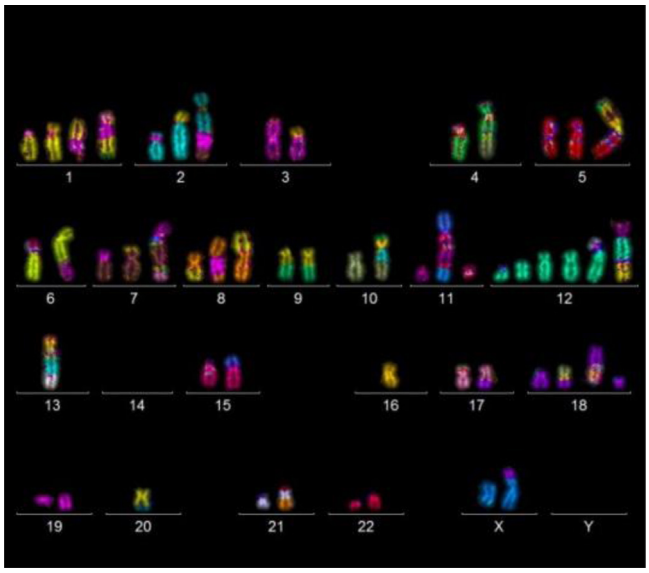

Fig. 4. Representative M-FISH image of a pseudo-coloured DMS53 karyotype.

an equi-fluence (1 track/nucleus) of α-particle-induced aberration complexity in peripheral blood lymphocytes (PBL) [7,12] and haemopoeitic stem cells (HSC) [28], where the S:C ratio was ~<1. Indeed, between 60 and 80% (depending on LET of the α-particle) of HSC or PBL which contained an exchange were classified as having at least one complex in comparison to only ~40% of NHBE cells (Fig. 1). This reduction in complexity may be a reflection of the relationship between the delayed formation of exchanges in heavily damaged cells [2,39–41] whereby exchanges of increasing complexity are observed at later sampling times [42]. However no evidence for this was found in NHBE cells (for more details see Themis et al. [27]). Therefore complex chromosome aberrations are not the dominant exchange-type in NHBE cells exposed *in vitro* to high-LET α-particle radiation in a set-up where the α-particles hit perpendicularly. The small proportion of non-G_1 cells present at the time of irradiation and/or differences in repair fidelity may be relevant but also pertinent is that NHBE cells are ellipsoid in shape and geometrically flatter than PBL or HSC. Thus, NHBE cells irradiated with a single α-particle through the base of the dish (as in this study), would be expected to have fewer chromosome territories intersected (and also fewer total DSB) compared to spherical nuclei (Fig. 1). Accordingly, these data support the proposal that in addition to radiation quality and dose, the complexity of aberrations initially induced by

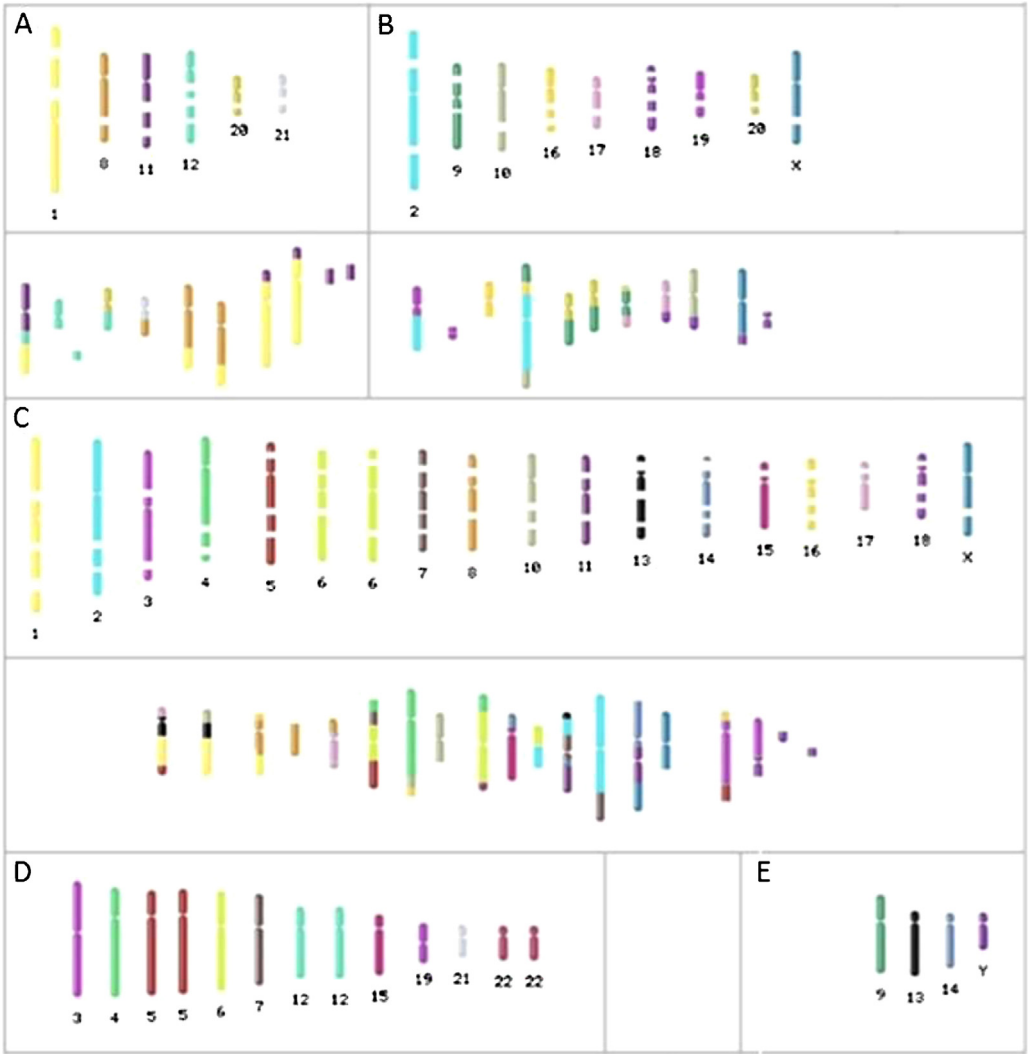

Fig. 5. Cartoon of DMS53 'cell 2' M-FISH karyotype. Groups of interacting chromosomes (A, B and C) are shown separately in two rows. The first row describes the break pattern assumed in each 'normal' chromosome while the second row shows the abnormal chromosomes observed by M-FISH. (D) identifies chromosomes classified as 'apparently normal' while (E) shows chromosomes "missing" from that spread.

particulate radiation is related to the number of chromosome territories (CTs) intersected by individual tracks [7,12]. Indeed a recent study demonstrates this directly by showing varying fractions of complex aberrations to be induced in AG1522 fibroblasts depending on the path of exposure through the ellipsoid nucleus [43].

The frequency of simple exchanges induced in NHBE cells after exposure to low-LET γ-rays is also lower than that previously observed in PBL (Table 1) [5,38,44,45]. Our results are more consistent with those observed in HF19 fibroblasts [46] inferring that cellular geometry and CT organisation may also be relevant for the induction of aberrations of varying complexity after γ-rays. The dynamics of damaged chromatin and the existence of specialised repair centres remain controversial [47,48] however a key aspect of the sequential exchange model for the formation of complex exchanges is that migration of initially induced damage is limited within localised nuclear regions. This is shown by the reduction in the sequential linking of independent exchange events (therefore reduction in complex aberrations) when the spatial distance in energy deposition along an α-particle track is increased (Fig. 1), and by each non-reducible rejoining cycle only involving up to a maximum of three different chromosomes [28]. Thus, the mobility of damaged chromatin is limited by its topological organisation within the nucleus, impacting on the likelihood that damage can participate in 'rejoining events' which are beyond an 'interacting distance' of ~>1 μm [13,49]. Accordingly for low dose exposures, damage induced in CTs that occupy peripheral positions within ellipsoid nuclei (*i.e.* where less of their CT surface neighbours another CT) may be too distant to interact with other damage for the efficient induction of an interchange (simple or complex). If valid then one might anticipate a greater proportion of intra- rather than inter-chromosomal exchanges for peripheral compared to interior positioned chromosomes [50]. In addition, it would further support the expectation that exchange aberrations are correlated by the combined surface area of neighbouring territories whereby exchange partners reflect nuclear organisation and territorial neighbourhoods [13,51–54].

It is well established that the interphase positions of CTs display non-random preferential positioning within the cell nucleus with a degree of variability between individual cells. For instance, it has been widely reported that chromosomes adopt a radial position based on gene density whereby gene-rich chromosomes occupy the interior of the nucleus in spherical nuclei [17,55]. Such an organisation has also been observed in non-spherical, flattened cells such as fibroblasts but in addition, the size of the chromosome has also been shown to be important [16,18]. However when one considers proliferative compared to non-proliferative cells and also cells at varying stages of differentiation or disease status, chromosome position can change, implying other factors such as transcriptional activity may be the dominant mechanism involved [30,29,56,57]. Our data for ellipsoid NHBE cells do not fit completely with size correlated positioning since there are larger and smaller chromosomes towards the nuclear periphery and the largest chromosome (chromosome 1) is in an intermediate nuclear location. The data do not fit a gene-density distribution either even though there are gene-poor chromosomes (chromosomes 13 and 18) towards the nuclear periphery and a gene-rich chromosome (chromosome 17) towards the nuclear interior, the other chromosomes that are located at the periphery and interior have intermediate density of genes (Fig. 2). Therefore our data may be consistent with the organisational grouping whereby active transcription has control over chromosome location. Interestingly, Mehta et al. [58] observed small chromosomes, in particular chromosomes 13 and 18, to change their locations in a rapid motor-dependant process when under reversible growth arrest (low serum) conditions, in keeping with previous observations that certain chromosomes were differentially positioned according to their proliferative status [29]. We examined this for NHBE cells co-staining chromosomes 9 and 18 with the cell proliferation marker anti-Ki-67. Overall though, no difference in positioning for either chromosome was observed between proliferative (Ki-67 positive) and non-proliferative (Ki-67 negative) cells (Fig. 2).

Three of the chromosomes tested (chromosomes 16, 17 and 21) were positioned to the interior of NHBE nuclei, which given the flattened, ellipsoid shape of the nucleus may increase the likelihood of them being neighbouring territories in interphase. Interestingly, chromosomes 16 and 21 were identified by SCHIP analysis [32] as non-randomly forming exchanges in NHBE cells more often than expected after exposure to ionising radiation (Table 3). In addition to this, we also identified exchanges between chromosomes (1;13), (9;17), (9;18) and (12;18) to occur more frequently than expected assuming randomness. Thus, we find evidence of cell type-specific chromosome associations in keeping with the identification of clusters of particular (but different) chromosomes reported by Cornforth et al. [22] and Arsuaga et al. [59]. However in contrast to the aforementioned studies, our radiation-induced pair-wise data-set for NHBE cells was extremely limited. Therefore to support these findings we performed 2-colour FISH analysis on three of the identified non-random pairs; (1;13), (9;17) and (16;21). 2D measurements (ImageJ software, NIH, www.rsb.info.nih.gov) of the minimum distance between the edge:edge boundaries of each chromosome pair show that, on average, at least one chromosome existed within <1 μm of another, indeed, CTs were visibly touching in ~60% of nuclei of each pair tested (Table 4 and Fig. 3). By contrast, although similar to other studies, homologous chromosome pairs were separated by distances of >3.5 μm [55,29]. Taken together, these data are consistent with the expectation that spatial proximity of CTs influences the preferential formation of particular chromosome exchanges [20,60,61].

We M-FISH karyotyped a small cell lung cancer (DMS53) cell line with the objective of identifying clonal aberrations that may reflect early rearrangements in carcinogenesis, and which may also demonstrate a mechanistic association between non-random exchange formation and interphase positioning of chromosomes in NHBE cells [20,57,60,62]. Although the karyotype was highly rearranged, meaning any correlations with our NHBE cell findings may just reflect the large number of exchanges detected (Figs. 4 and 5), we did find two interactions that involved chromosomes previously detected in radiation-induced aberrations. Specifically, the preferential involvement identified between chromosomes 9 and 17, and chromosomes 1 and 13 (Table 3) are also seen in the DMS53 karyotype as der(9)t(9;17), der(9)t(16;9;17), ace(1;13;10) and der(13)t(17;135) (Tables 6 and 7). In addition, chromosomes 9 and 17 and, 1 and 13 were shown by 2-colour FISH to exist as neighbours in ~60% of NHBE nuclei (Fig. 3). Accordingly, it is possible that a fraction of the exchanges observed in DMS53 reflect their preferential CT position in normal lung epithelial cells highlighting the possibility of unravelling mechanistically and clinically relevant non-random chromosome exchanges within cell/individual sub-sets [57,62]. That said, published karyotypes of different SCLC cell lines similarly show high levels of structural rearrangement and, although certain chromosomes are apparently more frequently involved in exchanges than others *e.g.* chromosome 1, the involvement of common pairs of chromosomes are seen only rarely [63,64]. For instance Ashman et al. karyotyped five SCLC lines, with each containing between 3 and 10 exchanges, yet only a few translocation pairs were identified in multiple lines *e.g.* two lines involved exchanges between chromosomes 9 and 16, interestingly also observed in DMS53 as der(2)t(9;16;2;10) and der(9)t(16;9;17) (Tables 6 and 7). Elucidating the occurrence of non-random chromosomal translocations in such highly rearranged genomes is therefore challenged by the limited number of SCLC lines currently karyotyped.

Table 6
M-FISH karyotype of DMS53.

Cell 1
47,X,+X,−Y,der(X)(X;18),del(Xq),der(1)t(1;11)x2,ace(1;13;10),+2,ace(2;6),der(2)t(2;12),der(2)t(7;2;12),der(2)t(9;16;2;10),der(3)t(16;3;5),der(4)t(4;10;16),+5,del(5q),+6,der(6)t(4;7;6;5),der(6)t(12;4;7;6;5),der(6)t(6;15),der(7)t(13;2;7;14;11),+8,der(8)(1;8)x2,der(8)t(16;8;1),−9,der(9)t(16;9;17),der(10)t(10;18),del(10q),der(11)t(11;12;1),ace(11q)x2,+12,der(12)t(12;15),ace(12;19;21),del(12q),−13,der(13)t(17;13′;1;5),−14,ace(14p),der(14;11)t(14;11;X),del(16q),der(17)t(17;18),del(17p),der(18)t(3;18),ace(18q),ace(18q)x2,der(19)t(2;19),der(19)t(7;19),ace(19q),ace(19q),der(20)t(9;20)x2,der(20)t(5;20)

Cell 2
47,X,+X,−Y,der(X)(X;18),del(Xq),der(1)t(1;11)x2,ace(1;13;10),ace(2;6),der(2)t(2;7),der(2)t(9;16;2;10),der(3)t(16;3;5),der(4)t(4;10;16),+5,+6,der(6)t(4;7;6;5),der(6)t(4;6;15),der(7)t(13;2;7;14;11),der(8)(1;8)x2,der(8)t(16;8;1),ace(8q),−9,der(9)t(16;9;17),der(10)t(10;18),del(10q),der(11)t(11;12;1),ace(11q)x2,+12,del(12q),ace(12q),−13,der(13)t(17;135),−14,der(14;11)t(14;11;X),der(15)(14;15),del(16q),der(17)t(17;18),der(17)t(8;17),der(18)t(3;18),del(18q),ace(18q)x2,der(19)t(2;19),ace(19q),der(20)t(9;20)x2,der(20)t(12;20),der(21)t(8;21)

Cell 3
47,X,+X,−Y,der(X)(X;18),der(X)t(X;16;10),der(1)t(1;11),ace(2;6),der(2)t(2;7),der(2)t(9;16;2;10),der(3)t(3;16),der(4)t(4;10),del(5q),ace(5;12),+6,der(6)t(4;7;6;5),der(6)t(6;15),der(6)t(6;18),der(7)t(13;2;7;14;11),+8,der(8)(1;8)x2,der(8)t(16;8;1),−9,der(9)t(16;9;17),der(10)t(10;18),del(10q),der(11)t(11;12;1),ace(11q)x3,+12,+12,ace(12;19;21),del(12q),del(12q),ace(12),−13,der(13)t(17;135),−14,der(14;11)t(14;11;X),der(15)(14;15),der(16)t(12;16),der(17)t(17;18),der(18)t(18;3;6),ace(18q),der(19)t(2;19),der(19)t(7;19),ace(19q),ace(19q),der(20)t(9;20)x2,der(21)t(8;21)

Cell 4
47,X,+X,−Y,der(X)(X;18),del(Xq),der(1)t(1;11),der(1)t(115),ace(1;13;10),ace(2;6),der(2)t(9;16;2;10),der(2)t(15;2;7),del(4q),der(5;20)t(5;20;12),ace(5;20),ace(5;21),+6,der(6)t(4;7;6;5),der(6)t(1;6),der(7)t(13;2;7;14;7),+8,der(8)(1;8),der(8)t(16;8;1),−9,ace(9;16),der(9)t(9;17),der(10)t(10;18),del(10q),der(11)t(11;12;1),ace(11q)x2,+12,der(12)t(12;16;19),del(12q),ace(12q)x2,−13,der(13)t(17;135),−14,der(14;11)t(14;11;X),der(15)(14;15),der(16)t(5;3;16;12),del(16q),der(17)t(10;17),der(17)t(17;18),del(18),ace(18q),der(19)t(2;19),der(19)t(7;19)x2,der(20)t(9;20),der(21)t(8;21),−22

Cell 5
47,X,+X,−Y,der(X)(X;18),del(Xq),der(1)t(1;11),der(1)t(115),ace(1;13;10),ace(2;6),der(2)t(7;2;12),der(2)t(9;16;2;10),−3,der(3)t(;16;3),del(4q),+6,der(6)t(4;7;6;5),der(6)t(1;6),−7,der(7)t(13;2;7;14;7),+8,der(8)(1;8)x2,der(8)t(16;8;1),−9,der(9)t(16;9;17),der(10)t(10;18),del(10q),der(11)t(11;12;1),ace(11q)x2,+12,der(12)t(12;16;19),ace(12;19;21),del(12q),ace(12),−13,der(13)t(17;135),−14,der(14;11)t(14;11;X),der(15)(14;15),der(16)t(5;3;16;12),del(16q),ace(16;13;5),der(17)t(17;18),der(17)t(10;17),del(18),ace(18q),der(19)t(2;19),der(19)t(7;19)x2,ace(19q),der(20)t(9;20)x2,der(20)t(5;20),der(21)t(8;21)

Cell 6
47,X,+X,−Y,der(X)(X;18),del(Xq),der(1)t(1;11),der(1)t(115),ace(1;13;10),ace(2;6),der(2)t(7;2;12),der(2)t(9;16;2;10),del(4q),del(5q),+6,der(6)t(4;7;6;5),der(6)t(1;6),−7,der(7)t(13;2;7;14;7),+8,der(8)(1;8)x2,der(8)t(16;8;1),−9,der(9)t(16;9;17),der(10)t(10;18),del(10q),der(11)t(11;12;1),ace(11q)x2,+12,der(12)t(12;16;19),ace(12;19;21),del(12q),ace(12),−13,der(13)t(17;135),−14,der(14;11)t(14;11;X),der(15)(14;15),der(16)t(5;3;16;12),del(16q),ace(16;17;5),der(17)t(17;18),der(17)t(10;17),del(18),der(19)t(2;19),der(19)t(7;19)x2,ace(19q),der(20)t(9;20)x2,der(20)t(5;20),der(21)t(8;21)

Cell 7
47,X,+X,−Y,der(X)(X;18),del(Xq),der(1)t(1;11)x2,ace(1;13;10),ace(2;6),der(2)t(2;7),der(2)t(9;16;2;10),der(3)t(3;16),ace(3;18),der(4)t(4;10),+5,der(5)t(5;8),+6,der(6)t(4;7;6;5),der(6)t(6;15),der(7)t(13;2;7;14;7),+8,der(8)(1;8)x2,der(8)t(16;8;1),−9,der(9)t(16;9;17),der(10)t(10;18),del(10q),der(11)t(11;12;1),ace(11q)x2,+12,der(12)t(12;2;21),−13,der(13)t(17;135),−14,der(14;11)t(14;11;X),der(15)(14;15),del(16q),der(17)t(17;18),der(17)t(10;17),del(18q),del(18q),der(19)t(2;19),der(19)t(7;19),ace(19q),ace(19q),der(20)t(9;20)x2,der(20)t(12;20;2)

Cell 8
47,X,+X,−Y,der(X)(X;18),del(Xq),der(1)t(1;11)x2,ace(1;13;10),ace(2;6),der(2)t(2;7),der(2)t(9;16;2;10),der(3)t(16;3;5),ace(3;18),der(4)t(4;10;16),der(5)t(5;15),+6,der(6)t(4;7;6;5),der(6)t(6;5),der(7)t(13;2;7;14;11),+8,der(8)(1;8)x2,der(8)t(16;8;1),−9,der(9)t(16;9;17),der(10)t(10;18),del(10q),der(11)t(11;12;1),ace(11q)x2,+12,ace(12;19;21),del(12q),ace(12q),−13,der(13)t(17;135),−14,der(14;11)t(14;11;X),der(15)(14;15),del(16q),der(17)t(17;18),del(17p),del(18q),del(18q),der(19)t(2;19),der(19)t(7;19),ace(19q),ace(19q),der(20)t(9;20)x2,der(21)t(8;21)

Cell 9
47,X,+X,−Y,der(X)(X;18),del(Xq),der(1)t(1;11)x2,ace(1;13;10),ace(2;6),der(2)t(2;7),der(2)t(9;16;2;10),der(3)t(16;3;5),ace(3;18;5),der(4)t(4;10;16),der(5)t(5;18),+6,der(6)t(11;4;7;6;5),der(6)t(6;15),der(7)t(13;2;7;14;11;5),+8,der(8)(1;8)x2,der(8)t(16;8;1),−9,der(9)t(16;9;17),der(10)t(10;18),del(10q),der(11)t(11;12;1),ace(11q)x2,+12,der(12)t(12;2;21),−13,der(13)t(17;135),−14,der(14;11)t(14;11;X),der(15)(14;15),del(16q),der(17)t(17;18),del(17p),ace(18q)x2,del(18q),del(18q),der(19)t(2;19),der(19)t(1;19),ace(19q),ace(19q),der(20)t(9;20)x2,der(20)t(12;20),der(21)t(8;21)

Cell 10
47,X,+X,−Y,der(X)(X;18),del(Xq),der(1)t(1;11)x2,ace(1;13;10),der(2)t(2;7),der(2)t(9;16;2;10),ace(2;14),der(3)t(3;16),ace(3;18),der(4)t(4;10),der(5)t(5;20),+6,der(6)t(4;7;6;5;2),der(6)t(6;15),der(7)t(13;2;7;14;11),+8,der(8)(1;8),der(8)t(16;8;1),ace(8q),−9,der(9)t(16;9;17),der(10)t(10;18),del(10q),der(11)t(11;12;1),ace(11q)x2,+12,del(12q),−13,der(13)t(17;135),−14,der(14;11)t(14;11;X),der(14)t(17;14;9;12),ace(9;14),der(15)(14;15),der(16)t(5;16),del(16q),der(17)t(17;18),der(17)t10;17),ace(18q)x2,del(18q),del(18q),der(19)t(2;19),der(19)t(7;19),ace(19q),ace(19q),der(21)t(21;12;9)

Cell 11
47,X,+X,−Y,der(X)(X;18),del(Xq),der(1)t(1;11)x2,ace(1;13;10),ace(2;6),der(2)t(2;7),der(2;3)t(10;2;3),der(3)t(3;16),der(4)t(4;10),+5,+6,der(6)t(4;7;6;5),der(6)t(6;15)x2,ace(6;9),der(7)t(5;7),+8,der(8)(1;8)x2,der(8)t(16;8;1),−9,der(7;9)t(17;9;7;14;11),der(10)t(10;18),del(10q),der(11)t(11;12;1),ace(11q)x2,+12,ace(12;19;21),del(12q),ace(12),−13,der(13)t(17;135),−14,der(14;11)t(14;11;X),der(16)t(16;2;13),del(16q),der(17)t(17;18),der(17)t(17;10;9),der(18)t(3;18),ace(18q),del(18q),der(19)t(2;19),der(19)t(7;19),ace(19q),der(20)t(9;20),der(20)t(12;20),ace(20),der(21)t(8;21)

Cell 12
47,X,+X,−Y,der(X)(X;18),del(Xq),der(1)t(1;11),ace(1;13;10),ace(2;6),der(2)t(2;7),der(2)t(9;16;2;10),der(3)t(3;16),der(4)t(4;11),der(4)t(4;10),+5,del(5q),+6,der(6)t(4;7;6;5),der(6)t(6;15),der(6)t(6;11),der(7)t(5;7),+8,der(8)(1;8)x2,der(8)t(16;8;1),−9,der(9)t(9;17),der(10)t(10;18),del(10q),der(11)t(11;12;1),ace(11q)x2,+12,ace(12;19;21),del(12q),ace(12),−13,der(13)t(17;135),−14,ace(14p),der(14;11)t(14;11;X),der(15)(14;15),der(16)t(162;13),del(16q),der(17)t(17;18),der(17)t(10;17),ace(17;2;14;11),der(18)t(3;18),del(18q),ace(18q),der(19)t(2;19),der(19)t(7;19),ace(19q),ace(19q),der(20)t(9;20)x2,der(21)t(5;21;8)

Karyotypes presented as ISCN (2009) nomenclature. Breakpoints are omitted due to the difficulty in assigning translocation breakpoints.

Table 7
Clonal chromosome exchanges observed in DMS53.

Clonal exchanges	Cell number											
	1	2	3	4	5	6	7	8	9	10	11	12
der(X)t(X;18)	X	X	X	X	X	X	X	X	X	X	X	X
der(1)t(1;11)	X	X	X	X	X	X	X	X	X	X	X	X
der(1)t(11;1;5)				X	X	X						
ace(1;13;10)	X	X		X	X	X	X	X	X	X	X	X
ace(2;6)	X	X	X	X	X	X	X	X	X		X	X
der(2)t(2;7)		X	X				X	X	X	X	X	X
der(2)t(7;2;12)	X				X	X						
der(2)t(9;16;2;10)	X	X	X	X	X	X	X	X	X	X		X
der(3)t(3;16)			X		X		X	X		X	X	X
der(3)t(16;3;5)	X	X						X	X			
ace(3;18)							X	X		X		
der(4)t(4;10)			X				X			X	X	X
der(4)t(4;10;16)	X	X						X	X			
der(6)t(1;6)				X	X	X						
der(6)t(4;7;6;5)	X	X	X	X	X		X	X			X	X
der(6)t(6;15)	X		X				X		X	X	X	X
der(7)t(13;2;7;14;11)	X	X	X					X		X		
der(7)t(13;2;7;14;7)				X	X	X	X					
der(7)t(5;7)											X	X
der(8)(1;8)	X	X	X	X	X	X	X	X	X	X	X	X
der(8)t(16;8;1)	X	X	X	X	X	X	X	X	X	X	X	X
der(9)t(9;17)				X								X
der(9)t(16;9;17)	X	X	X		X	X	X	X	X	X		
der(10)t(10;18)	X	X	X	X	X	X	X	X	X	X	X	X
der(11)t(11;12;1)	X	X	X	X	X	X	X	X	X	X	X	X
der(12)t(12;16;19)				X	X	X						
der(12)t(12;2;21)							X		X			
ace(12;19;21)	X		X		X	X		X			X	X
der(13)t(17;13;1;5)	X	X	X	X	X	X	X	X	X	X	X	X
der(14;11)t(14;11;X)	X	X	X	X	X	X	X	X	X	X	X	X
der(15)(14;15)		X	X	X	X	X	X	X	X	X		X
der(16)t(5;3;16;12)				X	X	X						
der(17)t(17;18)	X	X	X	X	X	X	X	X	X	X	X	X
der(17)t(10;17)				X	X	X	X			X		X
der(18)t(3;18)	X	X									X	X
der(19)t(2;19)	X	X	X	X	X	X	X	X	X	X	X	X
der(19)t(7;19)	X		X	X	X	X	X	X		X	X	X
der(20)t(9;20)	X	X	X	X	X	X	X	X	X		X	X
der(20)t(5;20)	X				X	X						
der(20)t(12;20)		X							X		X	
der(21)t(8;21)		X	X	X	X	X		X	X		X	

Table highlights (marked as X) all chromosome exchanges which were observed in two or more cells (clonal) from all abnormalities described in Table 6.

In conclusion, our findings highlight the importance of cellular geometry and CT organisation for the induction of aberrations of varying complexity after exposure to both low and high-LET radiation. We also provide evidence that certain chromosome pairs preferentially exist as interphase neighbours and that this physical proximity influences their likelihood of forming a chromosome exchange.

Conflict of interest statement

The authors declare that there are no conflicts of interest.

Acknowledgements

The authors are grateful to the Department of Health who supported this work through the Radiation Protection Programme (Contract RRX115).

References

[1] J.R. Savage, P.J. Simpson, FISH "painting" patterns resulting from complex exchanges, Mutat. Res. 312 (1994) 51–60.
[2] R.M. Anderson, S.J. Marsden, S.J. Paice, A.E. Bristow, M.A. Kadhim, C.S. Griffin, D.T. Goodhead, Transmissible and nontransmissible complex chromosome aberrations characterized by three-color and mFISH define a biomarker of exposure to high-LET alpha particles, Radiat. Res. 159 (2003) 40–48.
[3] M.P. Hande, T.V. Azizova, C.R. Geard, L.E. Burak, C.R. Mitchell, V.F. Khokhryakov, E.K. Vasilenko, D.J. Brenner, Past exposure to densely ionizing radiation leaves a unique permanent signature in the genome, Am. J. Hum. Genet. 72 (2003) 1162–1170.
[4] M.P. Hande, T.V. Azizova, L.E. Burak, V.F. Khokhryakov, C.R. Geard, D.J. Brenner, Complex chromosome aberrations persist in individuals many years after occupational exposure to densely ionizing radiation: an mFISH study, Genes Chromosomes Cancer 44 (2005) 1–9.
[5] B.D. Loucas, M.N. Cornforth, Complex chromosome exchanges induced by gamma rays in human lymphocytes: an mFISH study, Radiat. Res. 155 (2001) 660–671.
[6] B.D. Loucas, R. Eberle, S.M. Bailey, M.N. Cornforth, Influence of dose rate on the induction of simple and complex chromosome exchanges by gamma rays, Radiat. Res. 162 (2004) 339–349.
[7] R.M. Anderson, D.L. Stevens, D.T. Goodhead, M-FISH analysis shows that complex chromosome aberrations induced by alpha-particle tracks are cumulative products of localized rearrangements, Proc. Natl. Acad. Sci. U.S.A. 99 (2002) 12167–12172.
[8] M.N. Cornforth, Analyzing radiation-induced complex chromosome rearrangements by combinatorial painting, Radiat. Res. 155 (2001) 643–659.
[9] P.J. Simpson, D.G. Papworth, J.R. Savage, X-ray-induced simple, pseudosimple and complex exchanges involving two distinctly painted chromosomes, Int. J. Radiat. Biol. 75 (1999) 11–18.
[10] R.K. Sachs, A.M. Chen, P.J. Simpson, L.R. Hlatky, P. Hahnfeldt, J.R. Savage, Clustering of radiation-produced breaks along chromosomes: modelling the effects on chromosome aberrations, Int. J. Radiat. Biol. 75 (1999) 657–672.
[11] A.A. Edwards, J.R. Savage, Is there a simple answer to the origin of complex chromosome exchanges? Int. J. Radiat. Biol. 75 (1999) 19–22.
[12] R.M. Anderson, D.G. Papworth, D.L. Stevens, N.D. Sumption, D.T. Goodhead, Increased complexity of radiation-induced chromosome aberrations consistent with a mechanism of sequential formation, Cytogenet. Genome Res. 112 (2006) 35–44.

[13] R.K. Sachs, A.M. Chen, D.J. Brenner, Review: proximity effects in the production of chromosome aberrations by ionizing radiation, Int. J. Radiat. Biol. 71 (1997) 1–19.
[14] D.T. Goodhead, H. Nikjoo, Radiation track structure, Radioprotection 32 (1997) C1–C3.
[15] J.M. Bridger, P. Lichter, Analysis of mammalian interphase chromosomes by FISH and immunofluorescence, in: W.A. Bickmore (Ed.), Chromosome Structural Analysis: A Practical Approach, IRL Press, Oxford, UK, 1999.
[16] A. Bolzer, G. Kreth, I. Solovei, D. Koehler, K. Saracoglu, C. Fauth, S. Muller, R. Eils, C. Cremer, M.R. Speicher, T. Cremer, Three-dimensional maps of all chromosomes in human male fibroblast nuclei and prometaphase rosettes, PLoS Biol. 3 (2005) e157.
[17] S. Boyle, S. Gilchrist, J.M. Bridger, N.L. Mahy, J.A. Ellis, W.A. Bickmore, The spatial organization of human chromosomes within the nuclei of normal and emerin-mutant cells, Hum. Mol. Genet. 10 (2001) 211–219.
[18] H.B. Sun, J. Shen, H. Yokota, Size-dependent positioning of human chromosomes in interphase nuclei, Biophys. J. 79 (2000) 184–190.
[19] S. Kozubek, E. Lukasova, L. Ryznar, M. Kozubek, A. Liskova, R.D. Govorun, E.A. Krasavin, G. Horneck, Distribution of ABL and BCR genes in cell nuclei of normal and irradiated lymphocytes, Blood 89 (1997) 4537–4545.
[20] J.J. Roix, P.G. McQueen, P.J. Munson, L.A. Parada, T. Misteli, Spatial proximity of translocation-prone gene loci in human lymphomas, Nat. Genet. 34 (2003) 287–291.
[21] W.A. Bickmore, P. Teague, Influences of chromosome size, gene density and nuclear position on the frequency of constitutional translocations in the human population, Chromosome Res. 10 (2002) 707–715.
[22] M.N. Cornforth, K.M. Greulich-Bode, B.D. Loucas, J. Arsuaga, M. Vazquez, R.K. Sachs, M. Bruckner, M. Molls, P. Hahnfeldt, L. Hlatky, D.J. Brenner, Chromosomes are predominantly located randomly with respect to each other in interphase human cells, J. Cell Biol. 159 (2002) 237–244.
[23] M.R. Branco, A. Pombo, Intermingling of chromosome territories in interphase suggests role in translocations and transcription-dependent associations, PLoS Biol. 4 (2006) 780–788.
[24] D.T. Goodhead, D.A. Bance, A. Stretch, R.E. Wilkinson, A versatile Pu-238 irradiator for radiobiological studies with alpha-particles, Int. J. Radiat. Biol. 59 (1991) 195–210.
[25] E. Garimberti, S. Tosi, Fluorescence in situ hybridisation (FISH), in: J.M. Bridger, E.V. Volpi (Eds.), Fluorescence In Situ Hybridisation (FISH): Protocols and Applications, Springer, New York, USA, 2010.
[26] J.A. Croft, J.M. Bridger, S. Boyle, P. Perry, P. Teague, W.A. Bickmore, Differences in the localization and morphology of chromosomes in the human nucleus, J. Cell Biol. 145 (1999) 1119–1131.
[27] M. Themis, E. Garimberti, M.A. Hill, R.M. Anderson, Reduced chromosome aberration complexity in normal human bronchial epithelial cells exposed to low-LET γ-rays and high-LET α-particles, Int. J. Radiat. Biol. (2003), http://dx.doi.org/10.3109/09553002.2013.805889 (in press).
[28] R.M. Anderson, D.L. Stevens, N.D. Sumption, K.M. Townsend, D.T. Goodhead, M.A. Hill, Effect of linear energy transfer (LET) on the complexity of alpha-particle-induced chromosome aberrations in human CD34$^+$ cells, Radiat. Res. 167 (2007) 541–550.
[29] J.M. Bridger, S. Boyle, I.R. Kill, W.A. Bickmore, Re-modelling of nuclear architecture in quiescent and senescent human fibroblasts, Curr. Biol. 10 (2000) 149–152.
[30] J.M. Bridger, I.S. Mehta, M. Amira, A.J. Harvey, Rapid chromosome territory relocation by nuclear motor activity in response to serum removal in primary human fibroblasts, Genome Biol. 11 (2010).
[31] J.M. Bridger, I.R. Kill, P. Lichter, Association of pKi-67 with satellite DNA of the human genome in early G1 cells, Chromosome Res. 6 (1998) 13–24.
[32] S. Vives, B. Loucas, M. Vazquez, D.J. Brenner, R.K. Sachs, L. Hlatky, M. Cornforth, J. Arsuaga, SCHIP: statistics for chromosome interphase positioning based on interchange data, Bioinformatics 21 (2005) 3181–3182.
[33] M.J. Zeitz, L. Mukherjee, S. Bhattacharya, J.H. Xu, R. Berezney, A probabilistic model for the arrangement of a subset of human chromosome territories in WI38 human fibroblasts, J. Cell. Physiol. 221 (2009) 120–129.
[34] C. Heride, M. Ricoul, K. Kieu, J. von Hase, V. Guillemot, C. Cremer, K. Dubrana, L. Sabatier, Distance between homologous chromosomes results from chromosome positioning constraints, J. Cell Sci. 123 (2010) 4063–4075.
[35] S. Darby, D. Hill, A. Auvinen, J.M. Barros-Dios, H. Baysson, F. Bochicchio, H. Deo, R. Falk, F. Forastiere, M. Hakama, I. Heid, L. Kreienbrock, M. Kreuzer, F. Lagarde, I. Makelainen, C. Muirhead, W. Oberaigner, G. Pershagen, A. Ruano-Ravina, E. Ruosteenoja, A.S. Rosario, M. Tirmarche, L. Tomasek, E. Whitley, H.E. Wichmann, R. Doll, Radon in homes and risk of lung cancer: collaborative analysis of individual data from 13 European case-control studies, Br. Med. J. 330 (2005) 223.
[36] S. Darby, D. Hill, H. Deo, A. Auvinen, J.M. Barros-Dios, H. Baysson, F. Bochicchio, R. Falk, S. Farchi, A. Figueiras, M. Hakama, I. Heid, N. Hunter, L. Kreienbrock, M. Kreuzer, F. Lagarde, I. Makelainen, C. Muirhead, W. Oberaigner, G. Pershagen, E. Ruosteenoja, A.S. Rosario, M. Tirmarche, L. Tomasek, E. Whitley, H.E. Wichmann, R. Doll, Residential radon and lung cancer—detailed results of a collaborative analysis of individual data on 7148 persons with lung cancer and 14,208 persons without lung cancer from 13 epidemiologic studies in Europe, Scand. J. Work Environ. Health 32 (2006) 1–83.
[37] C.S. Griffin, S.J. Marsden, D.L. Stevens, P. Simpson, J.R. Savage, Frequencies of complex chromosome exchange aberrations induced by 238Pu alpha-particles and detected by fluorescence in situ hybridization using single chromosome-specific probes, Int. J. Radiat. Biol. 67 (1995) 431–439.
[38] B.D. Loucas, M. Durante, S.M. Bailey, M.N. Cornforth, Chromosome damage in human cells by gamma rays, alpha particles and heavy ions: track interactions in basic dose–response relationships, Radiat. Res. 179 (2013) 9–20.
[39] K. George, H. Wu, V. Willingham, Y. Furusawa, T. Kawata, F.A. Cucinotta, High- and low-LET induced chromosome damage in human lymphocytes: a time-course of aberrations in metaphase and interphase, Int. J. Radiat. Biol. 77 (2001) 175–183.
[40] S. Ritter, E. Nasonova, Y. Furusawa, K. Ando, Relationship between aberration yield and mitotic delay in human lymphocytes exposed to 200 MeV/u Fe-ions or X-rays, J. Radiat. Res. (Tokyo) 43 (Suppl.) (2002) S175–S179.
[41] S. Ritter, E. Nasonova, E. Gudowska-Novak, Effect of LET on the yield and quality of chromosomal damage in metaphase cells: a time-course study, Int. J. Radiat. Biol. 78 (2002) 191–202.
[42] R. Lee, S. Sommer, C. Hartel, E. Nasonova, M. Durante, S. Ritter, Complex exchanges are responsible for the increased effectiveness of C-ions compared to X-rays at the first post-irradiation mitosis, Mutat. Res. 701 (2010) 52–59.
[43] M. Durante, D. Pignalosa, J.A. Jansen, X.F. Walboomers, S. Ritter, Influence of nuclear geometry on the formation of genetic rearrangements in human cells, Radiat. Res. 174 (2010) 20–26.
[44] S. Ritter, R. Lee, S. Sommer, C. Hartel, E. Nasonova, M. Durante, Complex exchanges are responsible for the increased effectiveness of C-ions compared to X-rays at the first post-irradiation mitosis, Mutat. Res. Genet. Toxicol. Environ. Mutagen. 701 (2010) 52–59.
[45] S. Golfier, G. Jost, H. Pietsch, P. Lengsfeld, F. Eckardt-Schupp, E. Schmid, M. Voth, Dicentric chromosomes and gamma-H2AX foci formation in lymphocytes of human blood samples exposed to a CT scanner: a direct comparison of dose response relationships, Radiat. Prot. Dosim. 134 (2009) 55–61.
[46] K.A. George, M. Hada, L.J. Jackson, T. Elliott, T. Kawata, J.M. Pluth, F.A. Cucinotta, Dose response of gamma-rays and iron nuclei for induction of chromosomal aberrations in normal and repair-deficient cell lines, Radiat. Res. 171 (2009) 752–763.
[47] T. Neumaier, J. Swenson, C. Pham, A. Polyzos, A.T. Lo, P.A. Yang, J. Dyball, A. Asaithamby, D.J. Chen, M.J. Bissell, S. Thalhammer, S.V. Costes, Evidence for formation of DNA repair centers and dose–response nonlinearity in human cells, Proc. Natl. Acad. Sci. U.S.A. 109 (2012) 443–448.
[48] B. Jakob, J. Splinter, M. Durante, G. Taucher-Schoiz, Live cell microscopy analysis of radiation-induced DNA double-strand break motion, Proc. Natl. Acad. Sci. U.S.A. 106 (2009) 3172–3177.
[49] J.R. Savage, Insight into sites, Mutat. Res. 366 (1996) 81–95.
[50] M. Hada, Y. Zhang, A. Feiveson, F.A. Cucinotta, H.L. Wu, Association of inter- and intrachromosomal exchanges with the distribution of low- and high-LET radiation-induced breaks in chromosomes, Radiat. Res. 176 (2011) 25–37.
[51] H. Wu, M. Durante, J.N. Lucas, Relationship between radiation-induced aberrations in individual chromosomes and their DNA content: effects of interaction distance, Int. J. Radiat. Biol. 77 (2001) 781–786.
[52] C. Cremer, C. Munkel, M. Granzow, A. Jauch, S. Dietzel, R. Eils, X.Y. Guan, P.S. Meltzer, J.M. Trent, J. Langowski, T. Cremer, Nuclear architecture and the induction of chromosomal aberrations, Mutat. Res. 366 (1996) 97–116.
[53] R.M. Anderson, N.D. Sumption, D.G. Papworth, D.T. Goodhead, Chromosome breakpoint distribution of damage induced in peripheral blood lymphocytes by densely ionizing radiation, Int. J. Radiat. Biol. 82 (2006) 49–58.
[54] J.R. Savage, Cancer. Proximity matters, Science 290 (2000) 62–63.
[55] T. Cremer, C. Cremer, Chromosome territories, nuclear architecture and gene regulation in mammalian cells, Nat. Rev. Genet. 2 (2001) 292–301.
[56] I. Rajapakse, M.D. Perlman, D. Scalzo, C. Kooperberg, M. Groudine, S.T. Kosak, The emergence of lineage-specific chromosomal topologies from coordinate gene regulation, Proc. Natl. Acad. Sci. U.S.A. 106 (2009) 6679–6684.
[57] L.A. Parada, P.G. McQueen, T. Misteli, Tissue-specific spatial organization of genomes, Genome Biol. 5 (2004) R44.
[58] I.S. Mehta, M. Amira, A.J. Harvey, J.M. Bridger, Rapid chromosome territory relocation by nuclear motor activity in response to serum removal in primary human fibroblasts, Genome Biol. 11 (2010).
[59] J. Arsuaga, K.M. Greulich-Bode, M. Vazquez, M. Bruckner, P. Hahnfeldt, D.J. Brenner, R. Sachs, L. Hlatky, Chromosome spatial clustering inferred from radiogenic aberrations, Int. J. Radiat. Biol. 80 (2004) 507–515.
[60] M.N. Nikiforova, J.R. Stringer, R. Blough, M. Medvedovic, J.A. Fagin, Y.E. Nikiforov, Proximity of chromosomal loci that participate in radiation-induced rearrangements in human cells, Science 290 (2000) 138–141.
[61] J.J. Boei, J. Fomina, F. Darroudi, N.J. Nagelkerke, L.H. Mullenders, Interphase chromosome positioning affects the spectrum of radiation-induced chromosomal aberrations, Radiat. Res. 166 (2006) 319–326.
[62] L.A. Parada, P.G. McQueen, P.J. Munson, T. Misteli, Conservation of relative chromosome positioning in normal and cancer cells, Curr. Biol. 12 (2002) 1692–1697.
[63] J.N. Ashman, J. Brigham, M.E. Cowen, H. Bahia, J. Greenman, M. Lind, L. Cawkwell, Chromosomal alterations in small cell lung cancer revealed by multicolour fluorescence in situ hybridization, Int. J. Cancer 102 (2002) 230–236.
[64] M. Grigorova, R.C. Lyman, C. Caldas, P.A. Edwards, Chromosome abnormalities in 10 lung cancer cell lines of the NCI-H series analyzed with spectral karyotyping, Cancer Genet. Cytogenet. 162 (2005) 1–9.
[65] ISCN, in: L.G. Shaffer, M.L. Slovak, L.J. Campbell (Eds.), An International System for Human Cytogenetic Nomenclature, Karger in collaboration with Cytogenetic and Genome Research, Basel, Switzerland, 2009.